ARMA 20–1900

SAND2020-2682C

Deterministic Discrete Fracture Network (DFN) Model for the EGS Collab Project on the 4850 Level of the Sanford Underground Research Facility (SURF)

P. Schwering
Sandia National Laboratories, Albuquerque, NM, USA
T. Doe
DoeGeo, Seattle, WA, USA
W. Roggenthen
South Dakota School of Mines and Technology, Rapid City, SD, USA
G. Neupane
Idaho National Laboratory, Idaho Falls, ID, USA
H. Johnston
National Renewable Energy Laboratory, Golden, CO, USA
P. Dobson, C. Ulrich
Lawrence Berkeley National Laboratory, Berkeley, CA, USA
A. Singh
Stanford University, Stanford, CA, USA
N. Uzunlar, C. Reimers
South Dakota School of Mines and Technology, Rapid City, SD, USA
The EGS Collab Team[1]

This paper was prepared for presentation at the 54th US Rock Mechanics/Geomechanics Symposium held in Golden, Colorado, USA, 28 June-1 July 2020. This paper was selected for presentation at the symposium by an ARMA Technical Program Committee based on a technical and critical review of the paper by a minimum of two technical reviewers. The material, as presented, does not necessarily reflect any position of ARMA, its officers, or members. Electronic reproduction, distribution, or storage of any part of this paper for commercial purposes without the written consent of ARMA is prohibited. Permission to reproduce in print is restricted to an abstract of not more than 200 words; illustrations may not be copied. The abstract must contain conspicuous acknowledgement of where and by whom the paper was presented.

ABSTRACT: The EGS Collab is conducting hydraulic fracture stimulation and fluid circulation experiments in the Sanford Underground Research Facility (SURF) located in Lead, South Dakota. A total of eight 60m-long subhorizontal boreholes were drilled from the 4850 Level (~1.5 km below the ground surface) into the crystalline rock of this former mine. Six of these holes are used for geophysical monitoring, one is used for hydraulic fracture stimulation, and the remaining hole was designed as a production borehole that receives the water from the injection well via the induced and natural fracture system. The primary goal fracture network: these modeling methods are critical for the development of enhanced geothermal systems (EGS). This includes the prediction of rock behavior during fracturing and during an extended period of water flow between the parallel injection and

[1]J. Ajo-Franlin, T. Baumgartner, K. Beckers, D. Blankenship, A. Bonneville, L. Boyd, S. Brown, J.A. Burghardt, C. Chai, Y. Chen, B. Chi, K. Condon, P.J. Cook, D. Crandall, P.F. Dobson, T. Doe, C.A. Doughty, D. Elsworth, J. Feldman, Z. Feng, A. Foris, L.P. Frash, Z. Frone, P. Fu, K. Gao, A. Ghassemi, Y. Guglielmi, B. Haimson, A. Hawkins, J. Heise, C. Hopp, M. Horn, R.N. Horne, J. Horner, M. Hu, H. Huang, L. Huang, K.J. Im, M. Ingraham, E. Jafarov, R.S. Jayne, S.E. Johnson, T.C. Johnson, B. Johnston, K. Kim, D.K. King, T. Kneafsey, H. Knox, J. Knox, D. Kumar, M. Lee, K. Li, Z. Li, M. Maceira, P. Mackey, N. Makedonska, E. Mattson, M.W. McClure, J. McLennan, C. Medler, R.J. Mellors, E. Metcalfe, J. Moore, C.E. Morency, J.P. Morris, T. Myers, S. Nakagawa, G. Neupane, G. Newman, A. Nieto, C.M. Oldenburg, T. Paronish, R. Pawar, P. Petrov, B. Pietzyk, R. Podgorney, Y. Polsky, J. Pope, S. Porse, J.C. Primo, C. Reimers, B.Q. Roberts, M. Robertson, W. Roggenthen, J. Rutqvist, D. Rynders, M. Schoenball, P. Schwering, V. Sesetty, C.S. Sherman, A. Singh, M.M. Smith, H. Sone, E.L. Sonnenthal, F.A. Soom, P. Sprinkle, C.E. Strickland, J. Su, D. Templeton, J.N. Thomle, V.R. Tribaldos, C. Ulrich, N. Uzunlar, A. Vachaparampil, C.A. Valladao, W. Vandermeer, G. Vandine, D. Vardiman, V.R. Vermeul, J.L. Wagoner, H.F. Wang, J. Weers, N. Welch, J. White, M.D. White, P. Winterfeld, T. Wood, S. Workman, H. Wu, Y.S. Wu, E.C. Yildirim, Y. Zhang, Y.Q. Zhang, Q. Zhou, M.D. Zoback

Sandia National Laboratories is a multimission laboratory managed and operated by National Technology & Engineering Solutions of Sandia, LLC, a wholly owned subsidiary of Honeywell International Inc., for the U.S. Department of Energy's National Nuclear Security Administration under contract DE-NA0003525.

production boreholes. Understanding the results from the induced fracturing and flow is complicated by the presence of significant natural fractures that interact with the stimulation and/or flow pathways. The delineation and characterization of natural fractures is thus an important part of the project, and therefore a model of the Discrete Fracture Network (DFN) was developed on a deterministic basis. The DFN was populated using observations and interpretations integrated from drift (horizontal passageways that allow access in the underground) fracture mapping, analysis of core recovered from the eight boreholes, borehole televiewer logs, and observations of flow between and within boreholes and in the drift. The natural fracture system is dominated by a pervasive northwest-trending, steeply- dipping shear system that is identifiable in the drifts and the core. Hydraulic fracture stimulation, flow/tracer circulation tests, and geophysical monitoring revealed that the behavior of the injected water, and perhaps the growth of induced fractures, has been significantly influenced by the existing fractures identified in the DFN.

1. INTRODUCTION

The EGS Collab project is conducting experiments in the Sanford Underground Research Facility (SURF) to investigate rock behavior during hydraulic fracturing and to couple those observations with comprehensive modeling activities. A complete description of the project goals is presented in Kneafsey and others (2018). The large underground facility developed in crystalline rocks in northwestern South Dakota, USA, extends to a depth of 2.25 km but is only maintained to a depth of 1.5 km for the purposes of housing and servicing scientific investigations. Figure 1 is a geologic map showing the overall distribution of rocks in the SURF underground in the vicinity of the EGS Collab experiment area of a portion of the 4850 Level (1.5 km below the surface) near the experiment. The complexly folded metasedimentary rocks of the upper Poorman Fm., where the first EGS Collab experiment is developed, surround the Yates amphibolitic core of the major part of the structure. The three rock types shown in the figure include two that are Precambrian in age, the amphibolitic Yates unit and the Poorman phyllite, and one that is more recent Tertiary-age rhyolite. The oldest rock is the amphibolite unit, which consists of hornblende-plagioclase schist that was originally basalt prior to metamorphism (Caddey and others, 1991). The metasedimentary Poorman phyllite overlies the amphibolite unit and in the area of the EGS Collab experiment is a quartz-mica-carbonate phyllite with significant graphite content (~1%).

The area in Figure 1 which is marked as “Rhyolite Dike Swarm” is a zone that contains numerous rhyolite dikes, which trends in a northwesterly direction and which captures many, but not all, of the intrusive bodies on this level. This dike system can be traced through many of the levels exposed in the SURF underground, and the dikes can be seen at the surface where they become sills at the Precambrian-Cambrian contact (Noble, 1948). The dike swarm on the 4850 Level is also parallel to a major 1 km wide ductile shear zone which is known as the Homestake Deformation Zone (Caddey and others, 1990). The zone strikes 340^{o} and dips 50^{o} to the northeast and its eastern margin is ~550 m to the southwest of the EGS Collab experiment area.

2. PURPOSE OF THE EXPERIMENT

The current phase of the EGS Collab experiment is evaluating the effectiveness and validity of approaches to modeling of rock mechanics, fluid flow, and thermal processes during hydraulic fracturing and subsequent heat extraction. The project exercises the modeling in a small-scale testbed environment that is larger than the laboratory scale but smaller than a full-scale geothermal production site. This has been accomplished on the 4850 Level of SURF using induced hydraulic fracturing followed by an extended period of heat extraction from closely spaced boreholes that are separated by tens of meters (Figure 2). The testbed, however, is complicated due to the presence of existing natural fractures that can connect and interact with the induced fractures produced by the experiment. Therefore, an understanding of the original orientation of fractures is important to understand the behavior of the testbed. To provide a recognized basis for studies involving modeling a deterministic “Common” Discrete Fracture Network (CDFN) was prepared to allow comparisons to be made effectively using a consistent fracture geometry. The present CDFN refers only to the distribution of natural fractures. The geometry of the induced fractures and their relationship to the present CDFN will be described as the monitoring experiments continue to be analyzed (e.g., Schoenball and others, 2019).

3. BOREHOLE DESCRIPTIONS

All boreholes in the testbed were drilled with HQ dimensions yielding hole diameters of 96 mm (63.5 mm core diameters), and special care was taken to keep the boreholes as straight as possible. The testbed consisted of eight subhorizontal boreholes, nominally 60 m long, which were left uncased with the exception that the upper 6.1 m (20 ft) were cased with stainless steel (Figure 2). The boreholes were drilled from the West Drift, a

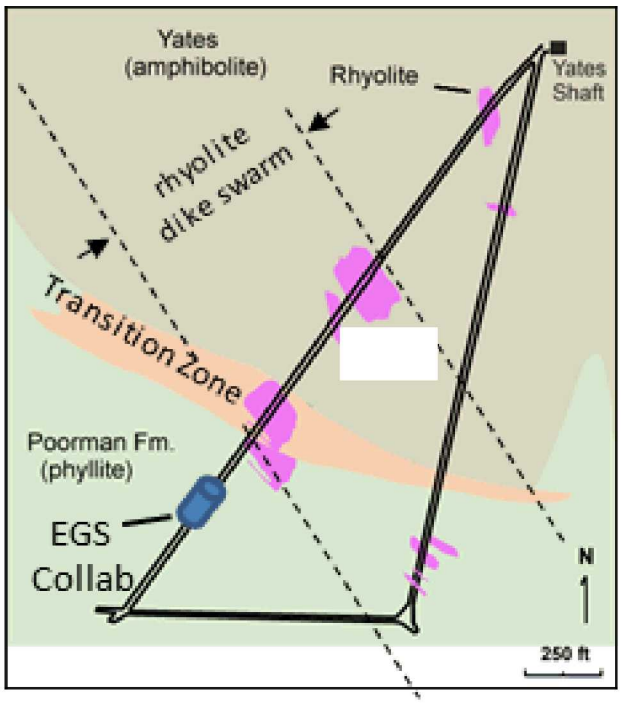

Figure 1. Geologic map of the 4850 Level of SURF near the Experiment 1 location of EGS Collab. The rhyolite dike swarm is a concentration of rhyolite dikes (depicted in pink) that trend to the northwest and dip at a high angle to the northeast. Other dikes are found outside of that zone, although they are not as numerous.

Table 1. Location and Orientation of the EGS Collab Borehole Collars in SURF Coordinates (ft) on the 4850 Level

Borehole	East	North	Elev. (MSL)	Measured Depth	Initial Direction (Trend)	Initial Plunge
E1-I	2669.9	-4414.9	380.0	63.4 m (208 ft)	356.3	-12.1
E1-P	2697.3	-4372.8	379.9	60.2 m (197.5 ft)	356.0	-12.7
E1-OB	2684.7	-4393.2	379.0	60.2 m (197.4 ft)	355.9	-28.0
E1-OT	2684.7	-4393.1	380.6	60.1 m (197.1 ft)	356.0	-6.0
E1-PST	2761.7	-4273.3	380.8	43.0 m (141.9 ft)	264.9	-4.8
E1-PSB	2761.5	-4273.6	379.3	60.0 m (197.0 ft)	260.3	-24.5
E1-PDT	2791.0	-4226.5	381.1	60.0 m (197.0 ft)	264.6	-5.2
E1-PDB	2791.0	-4227.0	379.7	60.4 m (198.1 ft)	261.3	-25.1

horizontal excavation, on the 4850 Level of SURF. Six of the boreholes are dedicated to geophysical monitoring, and the other two boreholes consist of an injector where the hydraulic fracturing was conducted, and a production borehole that was designed to receive the circulated water as part of the heat extraction experiment (Figure 2). The locations of the collars of the eight boreholes in SURF coordinates (ft) and the initial borehole trends and inclinations are listed in Table 1. Although only the initial inclinations are shown, the holes are relatively straight as can be seen in the perspective view of Figure 2. The induced hydraulic fractures produced during this experiment are shown in Table 2 along with the sequence of stimulations of these fractures.

The locations and orientations of the eight semi-horizontal 60-m long boreholes were designed using information derived from the nearby kISMET experiment (Oldenburg and others, 2017) that constructed five, closely spaced, subvertical boreholes, four of which were 50 m in length and one which was 100 meters in length. Hydraulic fracturing experiments in the long borehole produced a measurement of the orientation of the minimum compressive stress of N 2° E (corrected for magnetic north, Kneafsey and others, 2020) and a downward plunge of 9.3°. This information allowed the EGS Collab boreholes E1-I and E1-P to be constructed parallel to that stress direction. Therefore, the design plan was to produce induced fracturing in an east-west direction that is perpendicular to the injection borehole and would connect the injection (E1-I) and production (E1-P) boreholes.

Borehole orientations were measured during drilling using a gyrocompass tool beginning with a drill steel gyro compass and then transitioning to the relative-reading gyro tool when downhole. The downhole tool determined differences from the initial hole orientation during and after the completion of a borehole, however this data was supplemented by magnetic orientations from the downhole televiewer surveys when necessary. The gyro tool was chosen instead of only the magnetic measurements acquired during wireline logging due to the occurrences of sections of higher magnetic susceptibility. Although the downhole tool generally functioned well, the shallow inclination of the hole required more reliance on the gyro portion of the tool as opposed to the dip determinations. Consequently, errors tended to accumulate during the measuring process in some instances, perhaps due to a tendency for the gyro to be disturbed due to small bumps and disturbances during the logging process. The combination of magnetic determinations and the gyro determinations proved to be useful although the overall hole orientation had to be adjusted during the analysis of the seismic measurements due to the short standoff distances which require more accuracy than was available through the raw hole orientation measurements.

Table 2. Hydraulic fracture initiation locations along the axis of borehole E1-I on the 4850 Level of SURF (1.5 km depth).

Location of fracture along E1-I (measured depth from collar)	**Further Stimulation (in addition to hydraulic fracturing)**
39 m (128 ft)	Stimulation 3
43 m (142 ft)	Stimulation 2
50 m (164 ft)	Stimulation 1

as the fractures are stimulated by water flowing between the injector and the production boreholes.

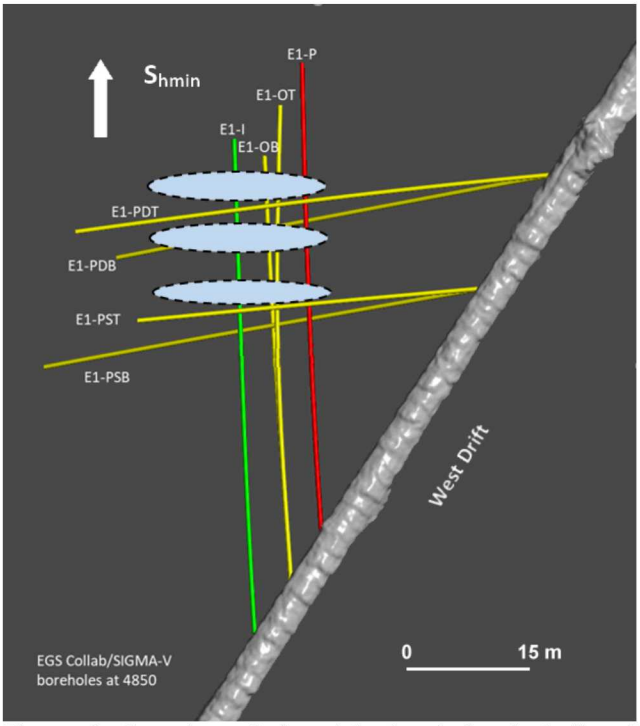

Figure 2. Location of the eight boreholes including E1-I (injection), E1-P (production), OT, OB, PSB, PST, PDT, and PDB. The predicted penny cracks (light blue discs) were designed to be perpendicular to the minimum compressive stress and to connect the injection and production borehole and are shown diagrammatically. The minimum compressive stress was assumed to be the same as the nearby kISMET determination of azimuth 002°, 9.3° downwards (Kneafsey and others, 2020; Oldenburg and others, 2017).

4. PROCESS OF DETERMINING THE COMMON DFN (CDFN)

The Common DFN (CDFN) model for the 4850 Level Phase 1 experiment was drawn together to provide an approximation of the fracture system that could be used for all of the modeling efforts to allow direct comparisons to be made. This CDFN is a deterministic approach as opposed to a statistical approach. It is anticipated that the CDFN will continue to evolve as interpretations become refined/integrated with new data and stochastic simulations, e.g. Wu and others (2019). Two types of fractures and fracture systems can be identified at the site, a) the natural fracture system prior to undergoing hydraulic fracturing and b) the fracture system after being artificially fractured. The latter consists of the natural system plus the induced system, although it also appears that the fracture system has continued to evolve through the course of the experiment, perhaps by fracture tension,

In order to characterize the natural fracture system, the data that was the most useful included geologic mapping of areas in the drifts where the natural fractures intersect the mine workings, core analysis, televiewer logs, and pumping of water to determine intersections of fractures with the well bores. After the hydraulic fracturing, delineation of the flow was imaged through a variety of geophysical techniques including microseismicity, continuous active source seismic, electrical resistivity tomography, and differential thermal analysis. It is anticipated that ongoing analysis of the geophysical data will further delineate the induced fracture system. Observations of water inflows using downhole video cameras as well as future actions, such as post-fracturing optical televiewer logging, are especially useful for direct observations of the final system.

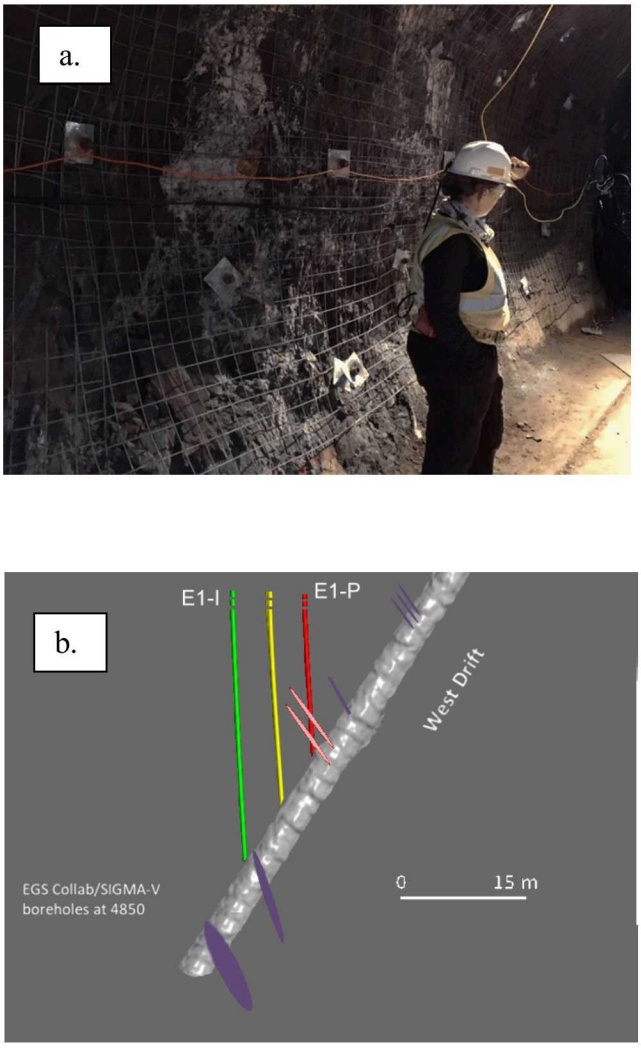

Figure 3.
a. Drift Weeps. Water that enters the drifts from the walls contains dissolved solids which remain as white encrustations in the drift.

b. These encrustations can be seen in the lower photo. The precipitates are often associated with linear features that can be traced from one side of the drift to the other and can provide orientation for the conductive features, as mapped in a. above, although free water is rarely observable.

4.1. Weeps

The intersection of postulated natural fractures with the drifts in the vicinity of the EGS Collab testbed is characterized by zones of white precipitate resulting from deposition of dissolved solids due to evaporation by the facility ventilation (Figure 3). These "weeps" have orientations that are generally parallel to the rhyolite zone and also to the large shear system to the southwest of the experiment area. Roggenthen and Doe (2018) showed that the intensity of the precipitates on the wall of the drift varies and that at least one major zone is located near the injection borehole. The weeps provide evidence of how the natural fracture system intersects the drift, and projection of the weep zones from the east side of the drift to the west side indicates the trend of the natural fracture system. The weep zones often are characterized by shearing, brecciation, and dissolution of the rock making up the zone.

4.2. Core Analysis

Examination of the entire suite of cores acquired during this phase of the experiment constituted an important tool for defining the natural fracture system. All boreholes had nearly 100 percent core recovery with excellent core quality. The wireline logging was registered to the top of casing, which required driller's core depths to be shifted to conform to that reference point. Although cores were photographed as they were acquired, analysis of natural fracturing was conducted over the succeeding months. This enabled the location of the natural fractures to be identified easily. Although the cores had many fractures, most were healed with a mixture of calcite and quartz. Several fractures were encountered that were open and clearly could conduct fluid. The open fractures fell into two categories: a) fractures that were clearly open and that sometimes had large crystals of calcite bridging the fracture aperture (Figure 4) and b) fractures that were lined and partially filled with potassium feldspar. The partially filled fractures were probably the result of hydrothermal activity and possibly shearing associated with the intrusion of the Tertiary-age rhyolite system. The Poorman Fm. country rock has significant amounts of carbonate, which lead to the development of partially dissolved structures resulting in a "wormy" appearance (Fig. 4). Characteristics of the natural fracture system were described by Roggenthen and Doe (2018) and Ulrich and others (2018), who examined core recovered during drilling of the testbed as well as the relationships of where postulated fractures intersected the drifts, known as weeps. Although the weeps in the vicinity of the experiment rarely show any free water, a major shear zone mapped in the Poorman Fm. to the southwest area of the site has dripping water associated with it. The major shear zone has a northwest trend and the rock is characterized by intensely sheared fabric in contrast to that found at Experiment 1. Roggenthen and Doe (2018) concluded that much, although not all, of the porosity in the deeper rock mass originated as a result of hydrothermal fluids associated with the intrusion of the nearby rhyolite bodies. The relationship with shearing, however, is somewhat uncertain because there is evidence that older shearing may have localized the rhyolite emplacement as well.

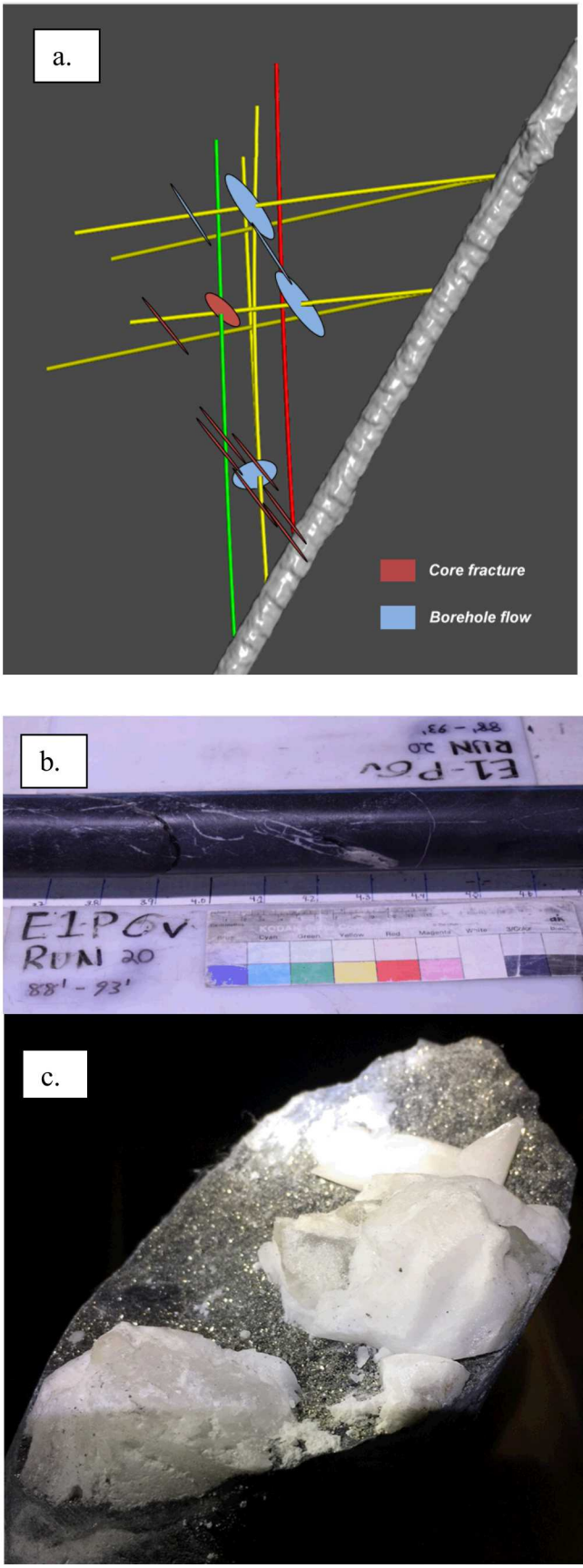

Figure 4.

a. Location of borehole intersections with visible open fractures and dissolution zones associated with shearing.

b. Photo of core from borehole E1-P showing a well-developed fracture.

c. Photo of core from borehole E1-P showing large calcite crystals with open-space growth.

4.3. Optical and Acoustic Televiewer Logging

Prior to the induced fracturing, optical and acoustic televiewer logs were run in all the boreholes, which provided a baseline to identify existing fractures. The acoustic televiewer proved to be the most useful for delineating existing fractures because it yielded the greatest contrast and was not affected by water clarity. The optical televiewer was useful for imaging bedding features and, in many instances, healed fractures when the water was sufficiently clear.

An example of the data derived from the optical televiewer is shown in Figure 5. The depth scale on the left of the figure is in meters from the collar and the next scale is in feet. The optical televiewer produces a diagram wherein the borehole is effectively unwrapped. This resulted in a sinusoidal pattern when planar fractures intersect the borehole. The borehole fracture pick is shown in relation to the entire core at the far right of the diagram with the tadpole plot showing the orientation of the fracture.

Based on the televiewer wireline data, potentially conductive fractures were identified. Figure 6 is a Fisher Distribution Plot showing that the fractures group well and have a northwesterly trend and a steep dip. For comparison, the overall trend and dip of the rhyolite zone is marked by the yellow star in the diagram based upon the work of Lisenbee and Terry (2009).

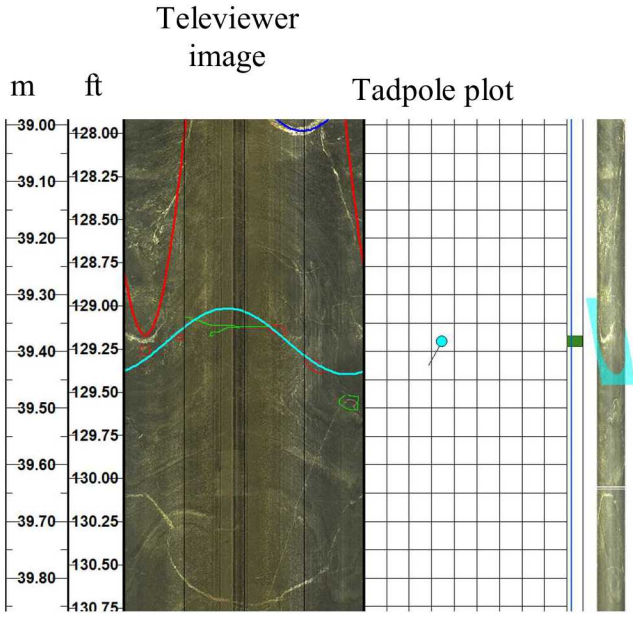

Figure 5. Example of an optical televiewer pick of apparent hydrofracture at 39.4 m (129.2 ft) measured depth, 210.4° azimuth, 34.5° dip.

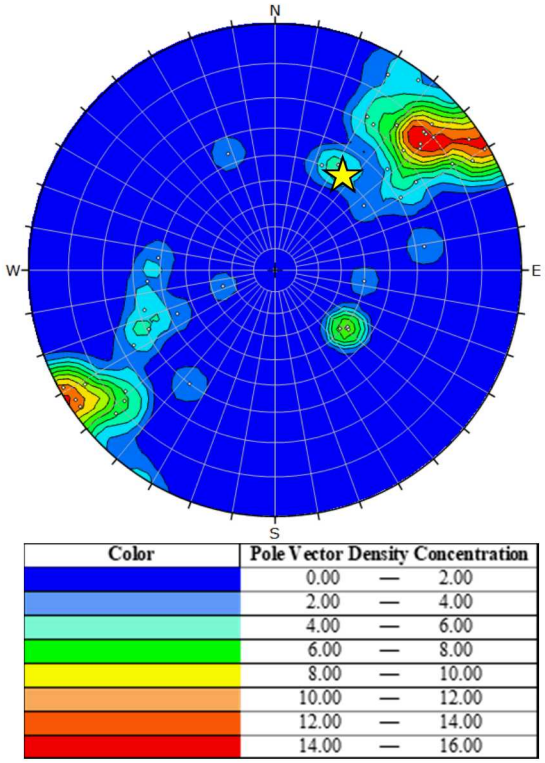

Figure 6. Fisher Distribution plot of the potentially conductive fractures identified from the televiewer data. The data shows a well-defined northwesterly trend for the steeply dipping fractures. The yellow star shows the approximate overall orientation of the rhyolite zone to the north of the site as shown in Figure 1.

4.4. 4.4 Downhole Video Camera

Prior to instrumentation and hydraulic fracture activities, a downhole camera was deployed to verify the presence and location of hydraulically productive natural fractures. Several natural fractures were observed to either a) naturally produce water in a borehole or b) produce water in one borehole when water was introduced to another (i.e., a fracture connecting two boreholes). One key fracture identified by this exercise intersected both the E1-P and E1-OT wells, dubbed the 'OT-P connector' (Figure 7). The robust hydraulic communication (i.e., could pour water into one well and watch the water come out of the other well nearly instantaneously), location, and orientation of this feature would together prove highly influential on post-stimulation hydraulic circulation tests (e.g., Kneafsey and others, 2020).

Pumping and stimulation of the fracture system were conducted after hydraulic fracturing. The stimulation may have created new sets of fluid pathways as intended, however, the existing natural fracture network influenced stimulated flow paths as well. In order to visualize at least a portion of the system, the downhole camera was operated during stimulation of the fracture system and was able to capture critical characteristics of fractures intersecting the production (E1-P) borehole. Although fractures in boreholes may appear to be a simple planar feature (e.g. Figure 5), the downhole camera showed that, in this instance, the system of natural pathways consists of pinholes occupying a fracture plane. In this case the entire semi-healed fracture plane was not in communication. Instead, small holes were the means by which the water entered the borehole (See the image in Figure 7 from the downhole camera in E1-P). This pinhole behavior probably is due to the history of shearing followed by partial healing within the natural fracture. This resulted in planar features with varying amounts of permeability. The fracture sets dominated by large apertures and voids, however, would not show this behavior.

5. DISCUSSION

The discrete fracture network that was derived from a variety of techniques including drift weeps, core analysis, televiewer logging, and downhole video is shown in Figure 8. The model was constructed in the Golder Fracman™ platform, which aided greatly in integrating the fracture observations into a unified framework. The model is a deterministic approach to approximating a system that is undoubtedly much more complex. For instance, several of the fractures in the system are shown

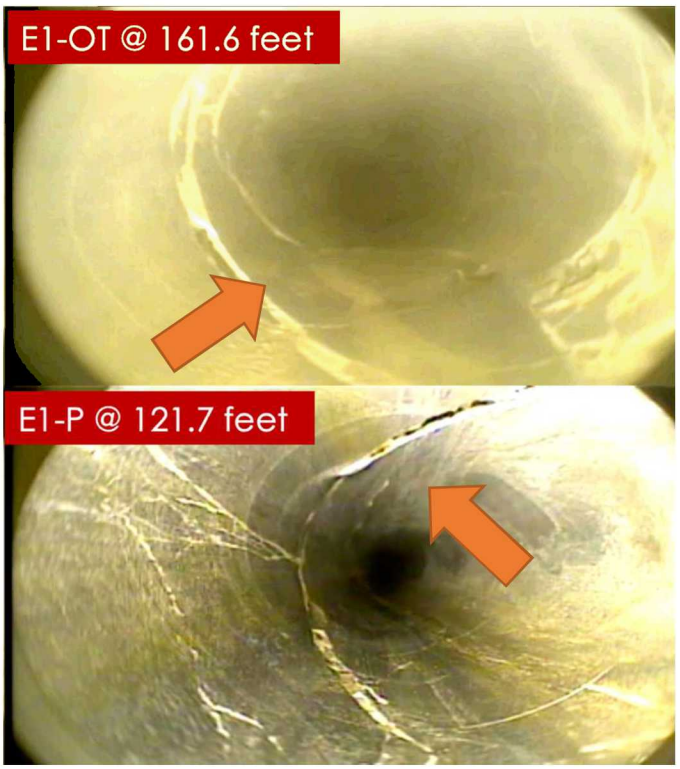

Figure 7. Downhole camera images of the OT-P connector. Arrows indicate observed water inflow locations.

as simple planes, and it is clear on the basis of the core examination that they represent zones with finite widths approaching 1 – 2 m in true thickness. Nevertheless, from the standpoint of providing a framework upon which more advanced modeling work can be built, this CDFN should provide a common basis to allow direct comparisons between different modeling approaches. The effect of minor changes in the composition of the rock in the dominant carbonate mica phyllite, including varying amounts of larger quartz inclusions, has not yet been determined. However, the upper holes tend to present more fracturing than the observation/monitoring holes drilled at steeper downward plunges, although the heterogeneity of the rock compositions may have an impact in that regard.

In general, the trend of the fracture system tends to parallel the rhyolite zone to the northeast, although the fractures in the EGS Collab Experiment 1 area appear to have somewhat higher dips (nearly vertical) than the rhyolite zone. The EGS Collab system also parallels a major shear to the southwest, but it is difficult to establish a clear genetic relationship between these three features, e.g. which occurred first and which might have influenced the orientation of the other features in the system. The metasedimentary rocks making up this area are tightly folded, and their fold axes also have a northwesterly trend. The model in Figure 8 shows several identifiable conductive zones, but the appearance of the fracture system depends upon the observation scale. Each of these zones probably has regions of varying fluid conductivity within them, but at larger scales, the entire area could be considered a single shear zone.

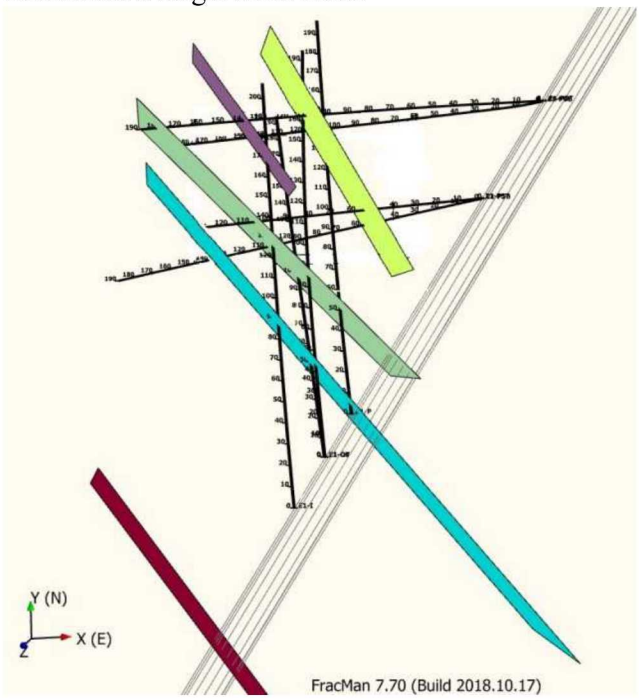

Figure 8. Model of a deterministic Common DFN based upon weeps exposed in the drift, potential conductors, and flowing fractures.

The geophysical monitoring instrumentation in the boreholes is an important source of information, but it is most useful in detecting the paths created by the hydraulic fracturing and subsequent flow through the combination of the natural fractures and the induced fractures. This information will be incorporated later when all geophysical data is available and other information, including tracer analyses (e.g. Mattson and others, 2019; Neupane and others, 2020) can be integrated.

Although the described model is an approximation of the geologic situation, it provides a common environment for modeling efforts to improve upon. Additional constraints on both the natural and induced systems will be provided by analysis of the large amount of geophysical data acquired from the monitoring boreholes, which acquired microearthquake data, continuous active source crosshole seismic, and electrical resistivity tomography (e.g., Schoenball and others, 2019; Chi and others, 2020, Johnson and others, 2019).

6.0 CONCLUSIONS

Several types of information related to fracture orientation, intensity, and history, such as core analysis, downhole logging, downhole video, and observations of the intersection of the natural fracture system with the

drift were applied the system. This allowed the identification and delineation of the steeply-dipping, northwest-trending fracture zones which, in turn, led to the development of a common discrete fracture network (CDFN) model. The model was constructed from the standpoint of a deterministic approach based upon these techniques. Analysis of the induced fractures developed during the hydraulic fracturing and the subsequent circulation of water were not considered but will be described as further analysis based upon the geophysical is completed.

The CDFN provides a basis for the modeling efforts to allow them to have a common starting point. As such, the baseline provides an important tool that will permit the modeling to be directly compared. This deterministic framework can be used as the basis for the development of stochastic fracture models for the test bed (e.g., Neupane and others, 2020).

7.0 ACKNOWLEDGMENTS

This material was based upon work supported by the U.S. Department of Energy, Office of Energy Efficiency and Renewable Energy (EERE), Office of Technology Development, Geothermal Technologies Office, under Award Number DE-AC02-05CH11231 with LBNL and other awards to other national laboratories. The United States Government retains, and the publisher, by accepting the article for publication, acknowledges that the United States Government retains a non-exclusive, paid-up, irrevocable, world-wide license to publish or reproduce the published form of this manuscript, or allow others to do so, for United States Government purposes. The research supporting this work took place in whole or in part at the Sanford Underground Research Facility in Lead, South Dakota. The assistance of the Sanford Underground Research Facility and its personnel in providing physical access and general logistical and technical support is gratefully acknowledged. The use of the Golder Fracman™ Viewer is appreciated. Some of the figures were generated using Leapfrog Software. Copyright © Seequent Limited. Leapfrog and all other Seequent Limited product or service names are registered trademarks or trademarks of Seequent Limited.

This paper describes objective technical results and analysis. Any subjective views or opinions that might be expressed in the paper do not necessarily represent the views of the U.S. Department of Energy or the United States Government.

8.0 REFERENCES

1. Caddey, S.W., R.L. Bachman, and R.P. Otto, 1990, "15 Ledge ore discovery, Homestake Mine, Lead, South Dakota," *Proceedings of the Fourth Western Regional Conference on Precious Metals and the Environment, Sept. 19-22, 1990*, p. 405-423.
2. Caddey, S.W., R.L. Bachman, T.J. Campbell, R.R. Reid, and R.P. Otto, 1991, The Homestake Gold Mine, An Early Proterozoic Iron-Formation-Hosted Gold Deposit, Lawrence County, South Dakota, *U. S. Geological Survey Bulletin 1857-J, Geology and Resources of Gold in the United States,* 67 p.
3. Chi, B., L. Huang, K. Gao, J. Ajo-Franklin, T.J. Kneafsey, and EGS Collab Team, 2020, Anisotropic Imaging of Created Fractures in EGS Collab Experiments Using CASSM Data, *PROCEEDINGS, 45th Workshop on Geothermal Reservoir Engineering Stanford University, Stanford, California.*
4. Johnson, T., C. Strickland, H. Knox, J. Thomle, V. Vermuel, C. Ulrich, T. Kneafsey, D. Blankenship, and the EGS Collab Team, 2019, EGS Collab Project Electrical Resistivity Tomography Characterization and Monitoring, PROCEEDINGS, 44th *Workshop on Geothermal Reservoir Engineering, Stanford University, Stanford. California.*
5. Kneafsey, T.J., D. Blankenship, P.F. Dobson, J.P. Morris, M.D. White, P. Fu, P.C. Schwering, J.B. Ajo-Franklin, L. Huang, M. Schoenball, T.C. Johnson, H.A. Knox, G. Neupane, J. Weers, R. Horne, Y. Zhang, W. Roggenthen, T. Doe, E. Mattson, C. Valladao, and the EGS Collab team, 2020, The EGS Collab Project: Learnings from Experiment 1, SGP-TR-216, *PROCEEDINGS, 45th Workshop on Geothermal Reservoir Engineering Stanford University, Stanford, California.*
6. Kneafsey, T.J., P. Dobson, D. Blankenship, J. Morris, H. Knox, P. Schwering, M. White, T. Doe, W. Roggenthen, E. Mattson, R. Podgorney, T. Johnson, J. Ajo-Franklin, C. Valladao, and the EGS Collab team, 2018, An Overview of the EGS Collab Project: Field Validation of Coupled Process Modeling of Fracturing and Fluid Flow at the Sanford Underground Research Facility, Lead, SD, SGP-TR-213*, PROCEEDINGS, 43rd Workshop on Geothermal Reservoir Engineering Stanford University, Stanford, California.*
7. Lisenbee, A.L. and M. Terry, 2009, Development of a 3-D structural geology model of Homestake's 4100 to 5000 levels at the proposed location of the large cavities*, SDSMT* Contract #09-05, May 21, 2009.
8. Mattson, E., G. Neupane, M. Plummer, A. Hawkins, Y. Zhang and the Collab Team, 2019, Preliminary Collab Fracture Characterization Results from Flow and Tracer Testing Efforts, SGP-TR-214, PROCEEDINGS, 44th *Workshop on Geothermal Reservoir Engineering, Stanford University, Stanford. California.*
9. Neupane, G., E.D. Mattson, M.A. Plummer, R.K. Podgorney, and the EGS Collab Team, 2020, Results of multiple tracer injections into fractures in the EGS Collab Testbed-1, SGP-TR-216, *PROCEEDINGS, 45th*

Workshop on Geothermal Reservoir Engineering Stanford University, Stanford, California.

10. Neupane, G., R.K. Podgorney, H. Huang, E.D. Mattson, T.J. Kneafsey, P.F. Dobson, M. Schoenball, J.B. Ajo-Franklin, C. Ulrich, P.C. Schwering, H.A. Knox, D.A. Blankenship, T.C. Johnson, C.E. Strickland, V.R. Vermeul, M.D. White, W. Roggenthen, N. Uzunlar, T.W. Doe, and the EGS Collab Team, 2019, EGS Collab Earth Modeling: Integrated 3D Model of the Testbed, *Geothermal Resources Council Transactions*, v. 43, 22 p.

11. Noble, J.A., 1948, High-potash dikes in the Homestake Mine, Lead, SD, *Geol. Soc. Am*., v. 59, p. 927-940.

12. Oldenburg, C.M., P.F. Dobson, Y. Wu, P.J. Cook, T.J. Kneafsey, S. Nakagawa, C. Ulrich, D.L. Siler, Y. Guglielmi, J. Ajo-Franklin, J. Rutqvist, T.M. Daley, J.T. Birkholzer, H.F. Wang, N.E. Lord, B.C. Haimson, H. Sone, P. Vigilante, W.M. Roggenthen, T.W. Doe M.Y., Lee, M. Ingraham, H. Huang, E.D. Mattson, J. Zhou, T.J. Johnson, M.D. Zoback, J.P. Morris, J.A. White, P.A. Johnson, D.D. Coblentz, J. Heise, 2017, Overview of the kISMET project on intermediate-scale hydraulic fracturing in a deep mine, ARMA 17-780, *51st US Rock Mechanics/Geomechanics Symposium, San Francisco, California, USA.*

13. Roggenthen, W.M. and T. W. Doe and the EGS Collab Team, 2018, Natural Fractures and Their Relations to the EGS Collab Project in the Underground of the Sanford Underground Research Facility (SURF), ARMA 18-1190, *52nd US Rock Mechanics/Geomechanics Symposium Seattle, Washington, USA, 11 p.*

14. Schoenball, M., J. Ajo-Franklin, D. Blankenship, P. Cook, P. Dobson, Y. Guglielmi, P. Fu, T. Kneafsey, H. Knox, P. Petrov, M. Robertson, P. Schwering, D. Templeton, C. Ulrich, T. Wood, and the EGS Collab Team, 2019, Microseismic monitoring of meso-scale stimulations for the DOE EGS Collab project at the Sanford Underground Research Facility. SGP-TR-214, PROCEEDINGS, 44th *Workshop on Geothermal Reservoir Engineering, Stanford University, Stanford. California.*

15. Ulrich, C., P.F. Dobson, T.J. Kneafsey, W.M. Roggenthen, N. Uzunlar, T.W. Doe, G. Neupane, R. Podgorney, P. Schwering, L. Frash, A. Singh, and the EGS Collab team, 2018, The distribution, orientation, and characteristics of natural fractures for Experiment 1 of the EGS Collab Project, Sanford Underground Research Facility, ARMA 18-1252, *52nd US Rock Mechanics/Geomechanics Symposium Seattle, Washington, USA, 8 p.*

16. Wu, H., P. Fu, J.P. Morris, E.D. Mattson, A.J. Hawkins, Y. Zhang, R.R. Settgast, F.J. Ryerson, and EGS Collab Team, 2019, Characterizing Fracture Flow in EGS Collab Experiment Based on Stochastic Modeling of Tracer Recovery, SGP-TR-214, PROCEEDINGS, *44th Workshop on Geothermal Reservoir Engineering, Stanford University, Stanford, California.*